Comparing ultrastructural changes in the rabbit chorioretinal complex after 577-nm and 532-nm laser photocoagulation

S.A. Fedchenko, Ophthalmologist, Post-grad Student, O.S. Zadorozhnyy, Cand Sc (Med), N.I. Molchaniuk, Cand Sc (Biol), Sen Res Fellow, A.R. Korol, Dr Sc (Med)

Filatov Institute of Eye Disease and Tissue Therapy

Odessa, Ukraine

E-mail: laserfilatova@gmail.com

Background: *There is no unanimously adopted approach to titrating laser parameters in subthreshold retinal laser photocoagulation without ophthalmoscopically visible fundus changes.*

Purpose: *To compare the ultrastructural changes in the rabbit chorioretinal complex after various modes of 577-nm and 532-nm laser photocoagulation.*

Materials and Methods: *Ten rabbits (20 eyes) were involved in the experimental study. Eight (10 eyes) of them underwent different modes of 577-nm or 532-nm laser photocoagulation, and were euthanized at postlaser days 1 (4 rabbits) or 14 (4 rabbits). Ultra-thin sections of their ocular tissue specimens were subjected to electron microscopy and assessed for the state of their choriocapillaries, RPE and photoreceptor cells. In addition, 2 intact rabbits (4 eyes) were used as controls for comparison.*

Results: *577-nm or 532-nm conventional RLPC resulted in damage to RPE cells, all photoreceptor compartments and choriocapillaries; 577-nm or 532-nm selective RLPC resulted in damage to RPE cells and photoreceptor outer and inner segments, and 577-nm micropulse RLPC with the power setting adjusted to 50% threshold resulted in damage mostly to apical aspects of RPE cells and photoreceptor outer segments.*

Conclusion: *577-nm micropulse RLPC with the power setting adjusted to 50% threshold is a more photoreceptor- and choriocapillaris-sparing approach compared to 577-nm or 532-nm conventional and selective RLPC, and can be used in clinical practice as a laser treatment approach with the least invasive effect on the chorioretinal complex.*

Keywords:

chorioretinal complex, laser radiation, ultrastructural changes

Introduction

Currently, it is considered that it is not necessary to damage all retinal layers in order to achieve therapeutic efficacy of laser [1-3]. Furthermore, conventional retinal laser photocoagulation (RLPC) is associated with the risk of side effects due to retinal pigment epithelium (RPE) atrophy or development of choroidal neovascularization [3, 4]. Development of subthreshold, or tissue-sparing, micropulse laser therapy techniques for the treatment of various central retinal disorders is consequently underway [1]. Authors vary in their approaches to performing 577-nm or 532-nm tissue-sparing micropulse retinal laser photocoagulation, including titration of laser power parameters [2-7]. We favor the approach to titration of laser parameters which consists in adjusting the threshold laser power in the micropulse mode before switching to therapeutic treatment with reduced laser power [7-9]. We believe, that, with this approach, the effect of subthreshold micropulse laser applied in the absence of visible retinal photocoagulation lesions becomes more predictable. The approach was mathematically grounded and its validity was experimentally confirmed [8, 9]. However, which ultrastructural changes occur in the chorioretinal complex (choriocapillaries, RPE, and photoreceptor cells) after subtrhreshold laser photocoagulation without ophthalmoscopically visible fundus changes is still to be found.

The purpose of this study was to compare the ultrastructural changes in the rabbit chorioretinal complex after various modes of 577-nm and 532-nm laser photocoagulation.

Materials and Methods

All animal experiments were performed in compliance with the Law of Ukraine on Protection of Animals from Cruel Treatment No. 3447-IV dated 21.02.2006 and European Convention for the Protection of Vertebrate Animals Used for Experimental and Other Scientific Purposes from the European Treaty Series (Strasbourg,

1986), and approved by a local Bioethics Committee of the Filatov Institute.

Ten Chinchilla rabbits (20 eyes) were involved in the experimental study which was performed at the vivarium of the Institute. They were housed and bred conventionally.

Each animal underwent biomicroscopy and ophthalmoscopy at baseline (before RLPC) and at days 1 and 14 after RLPC.

Prior to laser procedure, animals were anesthetized with thiopental sodium 10% (1.0 mL/kg, intramuscularly). Immediately thereafter, both eyes received a drop of proparacaine HCl (0.5%) for topical anesthesia. The pupils were dilated with atropine sulphate.

After RLPC, a drop of sulfacyl natrium 20% and a drop of Ofloxacin 0.3% were applied to each eye four times daily. Four rabbits were euthanized at day 1, and another 4 rabbits were euthanized at day 14 after laser treatment. Electron micrographs of normal rabbit choroid and retina from 2 intact rabbits (4 eyes) were used for comparison.

All procedures were performed by one surgeon, with central portion of Goldmann three mirror lens used to focus the aiming beam. The laser spot size was maintained at ~200 μm.

The 532-nm frequency-doubled ND-YAG laser (Alcon, Ophthalas 532 EyeLite Laser Photocoagulator) and the 577-nm Supra laser (Quantel Medical, Clermont-Ferrand, France) were used in the experimental study. As the former laser incorporates a resonator for 1,064-nm laser emission, the device cannot be operated in a free-running mode at exposure times less than 0.01 s, whereas the later is an Optically Pumped Semiconductor Laser (OPSL) having a subthreshold micropulse mode, which generates customizable trains of microsecond pulses.

To perform threshold photocoagulation, laser spots were applied at 0.1-s exposure time and placed close together in a staggered pattern. Laser power was adjusted until grade 1 burn (according to the L'Esperance's classification) was obtained at the site of laser exposure.

In selective RLPC, a ten-pulse train was applied (10 ms ON, 100 ms OFF) until barely visible photocoagulation lesions were placed along myelinated fibers. Thereafter, laser power was reduced until no photocoagulation lesions could be detected within a minute after exposure to laser.

In micropulse laser treatment, the laser was switched to the micropulse mode at 15% duty cycle (pulse train (burst time), 0.3 s; 0.17 ms ON, 1 ms OFF). Photocoagulation lesions were placed along myelinated fibers, and laser power was adjusted until grade 1 burn was obtained at the site of laser exposure, with a subsequent laser power reduction of 50% [8, 9].

Electron microscopy was performed at the Pathology and Electronic Microscopy Laboratory of the Filatov Institute. Ultra-thin sections were observed and photographed with a PEM-100-01 Transmission Electron Microscope (Selmi, Sumy, Ukraine).

Results

At day 1 after 532-nm or 577-nm threshold RLPC, the most severe damage to chorioretinal structures was observed. In the rabbit eye tissue sections obtained after 532-nm RLPC, non-uniform choriocapillary lumens were observed. At some sites, choriocapillary lumen content was electron transparent, whereas at the other sites, it was filled with flakes and red blood cells. Thinned portions of endotehilal cells were compact and flattened. RPE cells showed mainly destruction in the mid- and apical cell regions, and exhibited hydropic changes varying in severity. Apical aspects of some RPE cells were seen separated from mid-cell regions. At the site of laser-induced damage, intercellular PRC edema was observed at photoreceptor cell (PRC) outer (OS) and inner segments (IS), some OS were seen separated from mid-cell regions, rupture of IS was noted, and some PRC nuclei were damaged.

Dilated choriocapillaries and thinned endotehilal cells were observed at after threshold retinal photocoagulation with a 577-nm yellow laser. In addition, some RPE cells were destructed, and some of the membranes were vacuolated. The apical aspect of these cells with phagosomes and fragmented PRC OS was seen separated from mid-cell regions. The interreceptor matrix (IRM) contained fragmented RPE cells, and PRC OS and IS. PRC nuclei were also damaged.

At day 14 after 532-nm or 577-nm threshold RLPC, severe damage to chorioretinal structures was still observed.

At day 1 after 532-nm selective laser irradiation, less apparent destructive changes in chorioretinal structures were noted. Choriocapillaries were dilated, and their walls were markedly thinned. A portion of the RPE layer showed no cells. The IRM contained fragmented RPE cells, PRC OS and PRC IS. Some RPE cells maintained their basal regions, whereas their other structures were ruptured, cellular nuclei were contracted, and large displaced cytoplasmic fragments were seen. In less affected RPE cells, hydropic cytoplasmic changes prevailed and included destructive foci at local cellular sites. In the PRC outer segments, destructive foci, fragmented OS disks and membanes, and cellular detritus were found. Laser-induced structural changes in PRC OS and PRC IS varied from mild to severe, with hydropic changes being more pronounced than others. Most PRC nuclei were not damaged, leaving the potential for PRC to recover (Fig. 1). At day 14 after selective 532-nm laser irradiation, some cytoplasmic destruction was noted in some RPE cells. In most RPE cells, signs of recovery of basal and mid- cytoplasmic regions, and of their apical aspects (with the formation of phagosomes and, subsequently, phagolysosomes) were observed. Fragmented PRC inner and outer segments were registered, but PRC nuclei were maintained. At some sites, chorioretinal ultrastructure appeared completely recovered.

At day 1 after 577-nm selective laser irradiation, within the laser irradiation focus, some RPE cells showed damage to their mid- and apical regions (Fig. 2). The IRM was markedly edematous and contained fragmented membranes of outer-segment disks. The RPE cells having vacuolated appearance, with membrane structures throughout the cytoplasm, and destructed apical aspect were seen near the above structures. Fragmented photoreceptor outer segments were observed occupying spaces below mid-cell regions of maintained portions of the RPE cells. At the laser irradiation focus, intercellular PRC edema extended to the external limiting membrane, but PRC nuclei were not edematous (Fig. 2). At day 14 after selective 577-nm laser irradiation, signs of ultrastructural recovery were seen in most RPE cells. The cytoplasm of these cells contained numerous organelles like ribosomes, polysomes, elements of granular endoplasmic reticulum (GER) and of smooth endoplasmic reticulum (SEPE), and mitochondria. In these cells, both apical aspects and apical microvilli contacting photoreceptor outer segments were well developed. Generally, PRC ultrastructure appeared recovered.

At day 1 after 577-nm micropulse laser delivery with the power setting adjusted to 50% threshold, most RPE cells and adjacent choriocapillaries showed a nearly normal structure (Fig. 3). Some other RPE cells, however, showed damaged apical regions, with reduced numbers of microvilli and phagosomes, and hydropical changes in the organelles. Solitary broken cells were seen in the PRC layer, although adjacent photoreceptor cells were far less damaged (Fig. 3). At day 14 after 577-nm micropulse laser delivery with the power setting adjusted to 50% threshold, choriocapillaries showed some dilation but otherwise appeared nearly normal (Fig. 4). Most RPE cells appeared nearly normal. Solitary cells in the RPE layer showed destruction, mostly, in the apical aspect, and exhibited hydropic and finely vesicular cytoplasmic changes. Nonetheless, most RPE cells demonstrated recovery of cell structure, and showed increased numbers of phagocytized fragmented photoreceptor outer segments. All cell components of photoreceptor layer cells appeared well developed and had a normal ultrastructure (Fig. 4)..

Discussion

The development of selective RLPC techniques has been initiated in order to reduce damage induced by conventional RLPC in retinal photoreceptor cells [2, 10-12]. Roider and colleagues investigated the mechanism of the selective RPE damage induced by repetitive microsecond laser pulses in rabbits. It has been noted that selective damage to the RPE can be achieved with laser pulses shorter than the time needed for heat conduction to spread temperature rise to adjacent sites, but long enough to induce damage to target structures. Histology demonstrated substantial differences in outcomes between continuous wave (CW) laser photocoagulation of the retina and selective retinal laser photocoagulation. Severe damage to the RPE only was found in either of the two approaches used. In addition, after retinal exposure to repetitive short laser pulses, the photoreceptors were arranged normally, and no damage to most of them was observed; the choriocapillaries remained unaffected, and contained intact red blood cells. However, after threshold retinal photocoagulation, the photoreceptors were uniformly destroyed, and the choriocapillaries showed signs of damage [2, 11-12].

Pasyechnikova et al [10] developed a mathematical model for thermal processes induced by threshold and subthreshold (selective) RLPC in retinal tissues, which is important to get the idea on the nature of induced effects. When these processes are understood, one can titrate laser parameters to obtain optimal effect in each specific case [10]. In addition, Pasyechnikova et al [1, 13] developed a indirect selective laser photocoagulation technique providing a selective effect on the RPE at the macula, and a minimal effect on the retinal photoreceptors and choroid.

In the current study, we assessed ultrastructural changes in the rabbit chorioretinal complex after photocoagulation with 532-nm green laser or 577-nm yellow laser with similar parameters. The most prominent chorioretinal ultrastructural changes were found after threshold laser photocoagulation. These changes involved severe damage to RPE and photoreceptor cells both after the 532-nm laser and after 577-nm laser. Moreover, at day 14 after threshold laser photocoagulation, severe chorioretinal damage was still present within the laser irradiation focus. Therefore, 532-nm or 577-nm conventional threshold laser photocoagulation is followed by severe and irreversible changes to RPE and photoreceptor cells. At day 1 after 532-nm or 577-nm selective laser photocoagulation, less apparent chorioretinal damage was evident, with RPE cells and photoreceptor outer segments being most affected. However, by day 14, their ultrastructure practically recovered due to the high regenerative potential of RPE cells. In addition, unlike threshold RLPC, photoreceptor nuclei after selective RLPC were mostly intact, leaving the potential for PRC ultrastructure to recover.

Micropulse RLPC was found to be the most tissue-sparing. At day 1, the apical regions of RPE cells and photoreceptor outer segments were most affected. But by day 14, this damage was already absent, and in some RPE cells, compensatory and restorative processes were observed, with signs of the improved phagocytic function. In addition, a recovery of structural and functional interrelationship between RPE and photoreceptor outer segment layers occurred. It is likely that micropulse RLPC in some way stimulates chorioretinal structures, thus promoting fast recovery of RPE and photoreceptor cells.

Conclusions

First, 532-nm or 577-nm selective laser photocoagulation is followed by severe damage to and even breakage of RPE cells, and by alteration of photoreceptor cells (without nuclear involvement), with subsequent recovery of their ultrastructure by day 14.

Second, 577-nm micropulse RLPC with the power setting adjusted to 50% threshold resulted in damage mostly to apical aspects of RPE cells and photoreceptor outer segments, with subsequent recovery of their ultrastructure by day 14.

Third, 577-nm micropulse RLPC with the power setting adjusted to 50% threshold is a more photoreceptor- and choriocapillaris-sparing approach compared to 532-nm or 577-nm conventional and selective RLPC.

Finally, 577-nm micropulse RLPC with the power setting adjusted to 50% threshold can be used in clinical practice as a laser retinal treatment approach providing the least invasive effect on the chorioretinal complex.

References

1. Pasyechnikova NV, Naumenko VA, Katsan SV. [Efficacy of selective laser photocoagulation of the macular region for age-related maculopathy depending on the structure and function of the region]. Oftalmol Zh. 2006;2:4-9. Russian
2. Roider J, Brinkmann R, Wirbelauer C, et al. Subthreshold (retinal pigment epithelium) photocoagulation in macular diseases: a pilot study. Br J Ophthalmol. 2000;84(1):40–7
3. Youssef PN, Sheibani N, Albert DM. Retinal light toxicity. Eye (Lond). 2011 Jan; 25(1): 1–14
4. Gatsu MV, Gordeyeva MV. [Modern concepts of laser treatment of soft macular drusen]. Oftalmologicheskie vedomosti. 2014;7(1):72-81 Russian
5. Romanova TA. [The ultrastructural changes of the choroid and retinal pigment epithelium of rabbits after exposure to subthreshold lasers with 532nm, 577 nm, and 810 nm wavelengths using millipulse and micropulse laser modes]. Kharkivska khirurgichna shkola. 2014;4:74-9. Russian
6. Maia A. A New Treatment for Chronic Central Serous Retinopathy. Retina Today. 2010 Jan-Feb (1):1-3.
7. Scholz P, Ersoy L, Boon CJ, Fauser S. Subthreshold Micropulse Laser (577 nm) Treatment in Chronic Central Serous Chorioretinopathy. Ophthalmologica. 2015;234(4):189-94
8. Fedchenko SA, Zadorozhnyy OS, Molchaniuk NI, Korol AR. [Ultrastructural changes in the rabbit chorioretinal complex following 577-nm laser photocoagulation]. Oftalmol Zh. 2017;4:51-5. Russian
9. Semenyuk V. Thermal interaction of multi-pulse laser beam with eye tissue during retinal photocoagulation: Analytical approach. Int J Heat Mass Transf. 2017;112(1):480-488
10. Pasyechnikova NV. [Theoretical and clinical study of the efficacy of laser treatment for retinal disorders] [Dr. Sc. (Med) dissertation]. Odesa: Filatov Institute of Eye Disease; 2003. 312 p. Russian
11. Roider J, Michaud NA, Flotte TJ, Birngruber R. Response of the retinal pigment epithelium to selective photocoagulation. Arch Ophthalmol. 1992 Dec;110(12):1786-92.
12. Roider J, Michaud N, Flotte T, Birngruber R. Histologie von Netzhautläsionen nach kontinuierlicher Bestrahlung und nach selektiver Mikrokoagulation des retinalen Pigmentepithels. Ophthalmologe. 1993 Jun;90(3):274–8
13. Pasyechnikova NV, Ivanytska OV, Katsan SV. [Optimizing the management of patients with macular drusen in age-related maculopathy]. Naukovyi visnyk Uzhgorods'kogo universitetu. 2004;22:75-78. Ukrainian

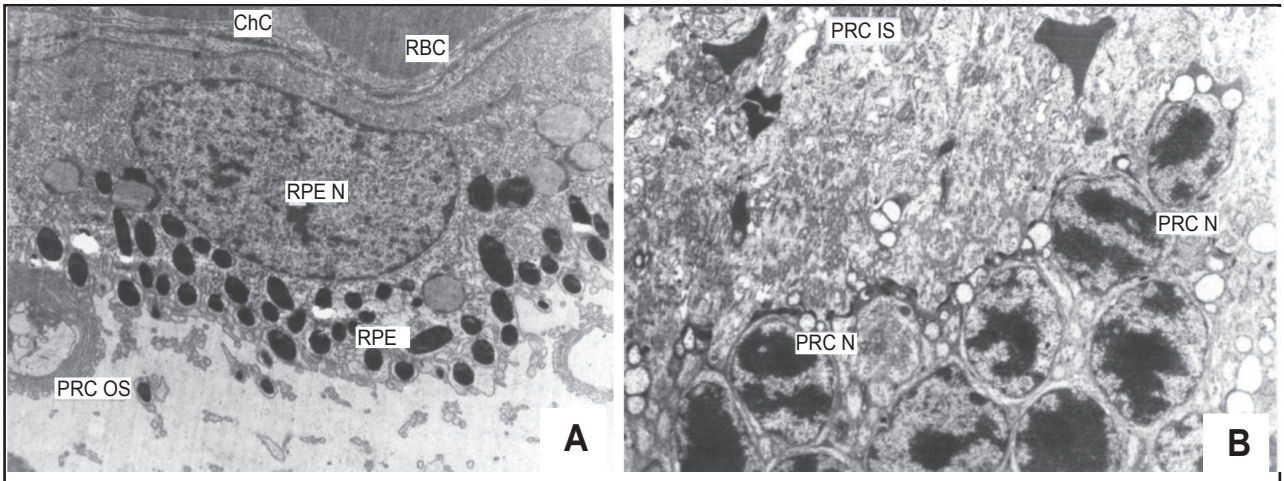

Fig. 1. Electron micrograph of rabbit's chorioretinal ultrastructure at day 1 after conventional 532-nm selective retinal laser photocoagulation. A. Enlarged choriocapillary lumens are observed and apical aspects of some RPE cells are seen separated from mid-cell regions. Original magnification ×3,000. B: Nearly normal ultrastructure of photoreceptor nuclei and cytoplasmic organelles. Original magnification ×3,000. Notes: PRC OS, photoreceptor outer segments; ChC, choriocapillaries; RBC, red blood cell; RPE, retinal pigment epithelium; RPE N, RPE cell nucleus; PRC N, photoreceptor nuclei; PRC IS, photoreceptor inner segments.

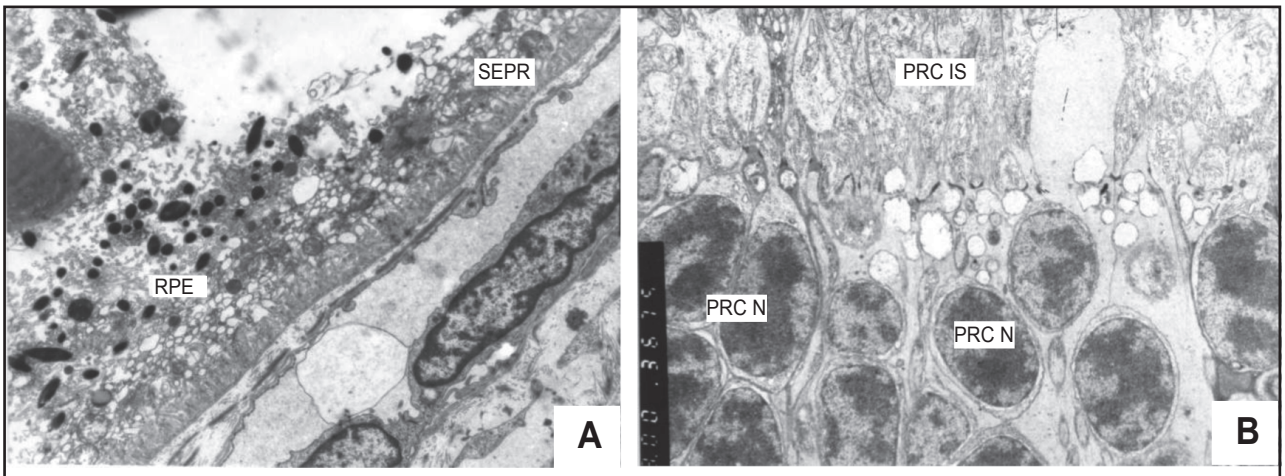

Fig. 2. Electron micrograph of rabbit's chorioretinal ultrastructure at day 1 after 577-nm selective retinal laser photocoagulation. A: Destruction of the apical region site of an RPE cell. Original magnification ×4,000. B: Destruction of a solitary photoreceptor cell (with nuclear involvement). Original magnification ×3,000. Notes: RPE, retinal pigment epithelium; SEPR, smooth endoplasmic reticulum; PRC N, photoreceptor nuclei; PRC IS, photoreceptor inner segments.

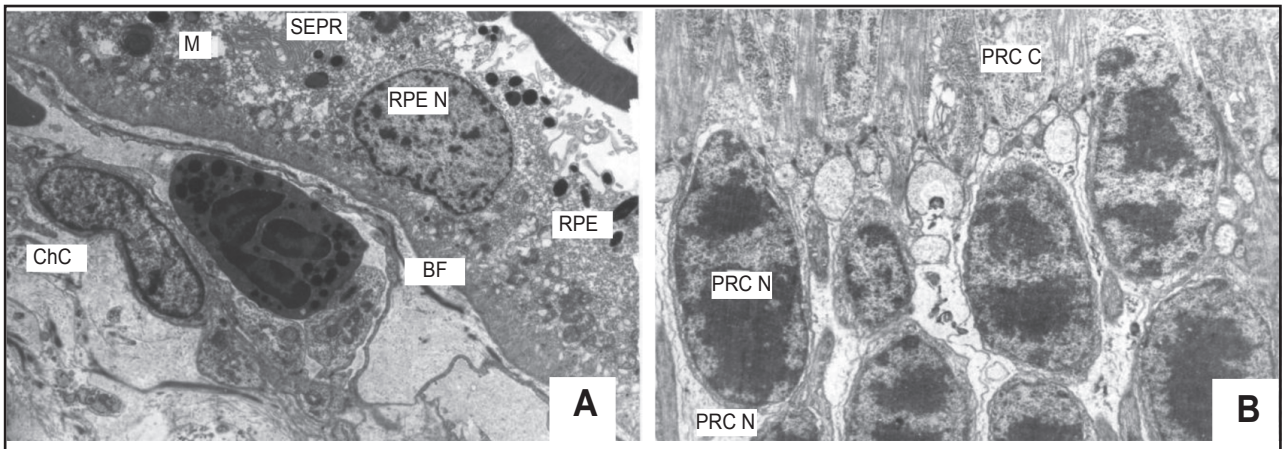

Fig. 3. Electron micrograph of rabbit's chorioretinal ultrastructure at day 1 after 577-nm micropulse retinal laser photocoagulation with the power setting adjusted to 50% threshold. A: Destruction of the apical region site of RPE cell and photoreceptor outer segments. Original magnification ×4,000. B: Normal cytoplasmic and nuclear ultrastructure of photoreceptor cells. Original magnification ×4,000. Notes: ChC, choriocapillaries; RPE, retinal pigment epithelium; RPE N, RPE cell nucleus; M, mitochondria; BF, basal folds; SEPR, smooth endoplasmic reticulum; PRC, photoreceptor cells; PRC N, photoreceptor nucleus; PRC C, photoreceptor cytoplasm.

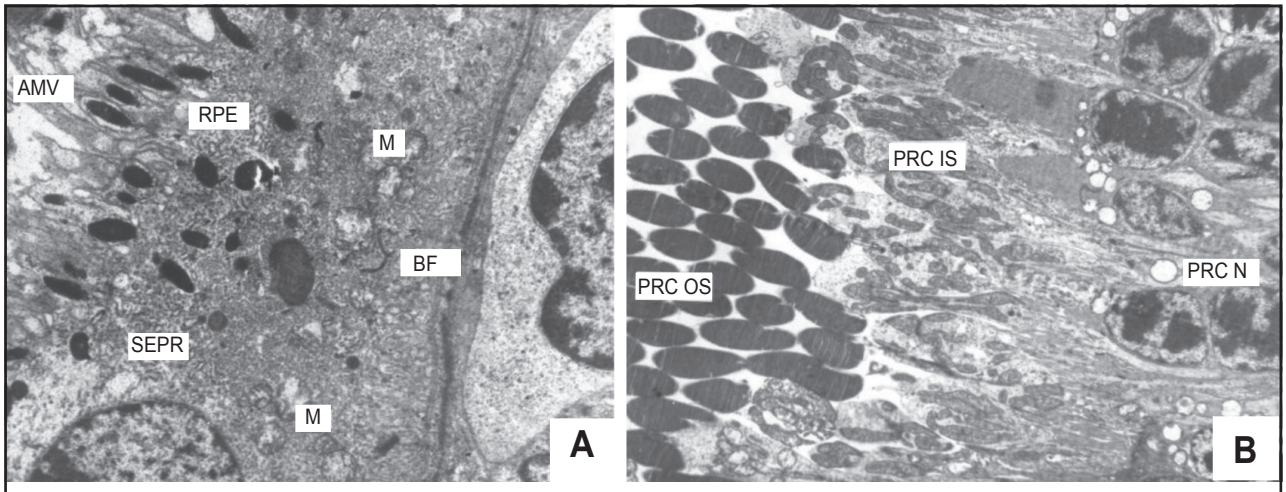

Fig. 4. Electron micrograph of rabbit's chorioretinal ultrastructure at day 14 after 577-nm micropulse retinal laser photocoagulation with the power setting adjusted to 50% threshold. A: Signs of compensatory and restorative processes are observed in a RPE cell, with increased abundance of smooth endoplasmic reticulum, granular endoplasmic reticulum, phagosomes, lysocomes and apical microvilli. Original magnification ×8,000. Notes: RPE, retinal pigment epithelium; AMV, apical microvilli; SEPR, smooth endoplasmic reticulum; BF, basal folds; M, mitochondria; PRC N, photoreceptor nuclei; PRC IS, photoreceptor inner segments; PRC OS, photoreceptor outer segments.